

# Field-Assisted Sintering of Nb–Al<sub>2</sub>O<sub>3</sub> Composite Materials and Investigation of Electrical Conductivity

Bastian Kraft,\* Susanne Wagner, Karl G. Schell, and Michael J. Hoffmann

Field-assisted sintering technique (FAST) is used for the preparation of Nb–Al<sub>2</sub>O<sub>3</sub> composite materials. The electrical conductivity is investigated depending on the particle size of the used starting powders and under varying volume contents of the refractory metal in the starting powder mixture. The percolation threshold is investigated and found to be influenced not only by the metal fraction but also by the particle size of the alumina used for sample preparation. For the fine- and coarse-grained alumina, a percolation threshold of 17.5 and 10 vol% Nb is estimated, respectively. Furthermore, the microstructure is investigated to gain a basic understanding of the dependency between microstructural features and the resulting material properties on the macroscopic scale. Also, the influence of the sintering process and the resulting microstructure–properties relationship is considered. It could be shown that the electrical properties are anisotropic because of anisotropy effects caused by the FAST process.

FAST is used for sample preparation from powder mixtures consisting of the electrically conductive refractory metal niobium and the insulating material alumina with different compositions.

The sintered samples are investigated to study the influence of powder composition and alumina particle size on densification, percolation threshold, and microstructural features. The percolation threshold is the changing point, where a composite switches from insulating to electrically conductive by varying the ratio of the conductive and insulating phase. At this point, a connected network of conducting phase is formed throughout the material.<sup>[5]</sup> In terms of the ever-growing demand for materials with specifically designed properties, the electrical properties are of great

## 1. Introduction

A basic understanding of the relationship between microstructural features and the material properties on the macroscopic scale is a fundamental field of materials research and was considered for Nb–Al<sub>2</sub>O<sub>3</sub> composite materials consolidated using field-assisted sintering technique (FAST).

FAST is a pressure-assisted sintering process that offers the opportunities of short processing times, high heating rates, and high densification of materials like refractories, that cannot be reached with conventional sintering technologies.<sup>[1,2]</sup> Sintering of materials is achieved by applying a current and uniaxial pressure by an electrically conductive mechanical loading system during the sintering process. The heating is caused by Joule heating which means that for electrically conductive materials, the heat is generated within the material itself and for electrically insulating materials within the pressing tool of the FAST system surrounding the compacted powder.<sup>[2–4]</sup> In this study,

interest. By applying an electrical voltage it is possible, for example, to influence the wetting behavior of components like casting channels and by this increasing the efficiency of processing.<sup>[6–10]</sup>

This study is part of an interdisciplinary research project on a new approach to develop coarse-grained refractory composite materials from presynthesized granules, recently introduced in several publications.<sup>[10–13]</sup> Such materials have the advantage of low shrinkage, good thermal shock and creep resistance, and tailorable properties for high-temperature applications.<sup>[10,12,13]</sup>

## 2. Experimental Section

### 2.1. Starting Materials

Niobium powder from EWG Wagner, Weissach, Germany, and the two different alumina powders 1) Alumina CT9FG (Almatis GmbH, Ludwigshafen, Germany), referred to as CT9FG, and 2) Treibacher Alodur WRG (Imerys Fused Minerals Zschornowitz GmbH, Gräfenhainichen, Germany), referred to as Alodur, with different particle size distributions were used for sample preparation. The different particle size distributions were measured by laser diffraction and dynamic image analysis method using a 1064 by CILAS and a Bettersizer S3 Plus particle size analyzer, making it possible to measure a very wide range of particle sizes. The starting powders were also analyzed using laser scanning microscopy (Keyence VK-X200 series) and scanning electron microscopy (SEM) (Nova NanoSEM 450 FEI).

From the starting powders, different Nb–Al<sub>2</sub>O<sub>3</sub> compositions were produced in a dry mixing process using a Turbular Tumbler type T2C (from WAB AG Maschinenfabrik, Basel, Switzerland).

B. Kraft, S. Wagner, K. G. Schell, M. J. Hoffmann  
Karlsruhe Institute of Technology  
IAM-Ceramic Materials and Technologies  
Haid-und-Neu-Str. 7, 76131 Karlsruhe, Germany  
E-mail: bastian.kraft@kit.edu

 The ORCID identification number(s) for the author(s) of this article can be found under <https://doi.org/10.1002/adem.202200063>.

© 2022 The Authors. Advanced Engineering Materials published by Wiley-VCH GmbH. This is an open access article under the terms of the Creative Commons Attribution License, which permits use, distribution and reproduction in any medium, provided the original work is properly cited.

DOI: 10.1002/adem.202200063

Here, the amounts of the starting powders for the desired compositions were filled into a polyethylene (PE) bottle and were mixed without addition of further additives or media for 10 min. The niobium volume content was varied between 7.5 and 100 vol % (7.5, 10, 12.5, 15, 17.5, 20, 40, 60, 80 vol% niobium).

## 2.2. Sample Preparation

After dry mixing the powders, samples were prepared using a field-assisted sintering system type HP D 25/1 from FCT Systeme GmbH, Frankenblick, Germany. The punch-die-setup used in the FAST system was made from graphite. The upper punch had a centered borehole stopping 5 mm short from the pressurized surface for temperature measurement with a pyrometer during the sintering process. An additional graphite foil was placed between the processed powders and the contacting surfaces of the tools to ensure good thermal and electrical contact. The samples were sintered temperature controlled with a heating rate of 100 K min<sup>-1</sup> from room temperature to 1600 °C, followed by a dwell time of 5 min, while during the dwell time, an axial pressure of 50 MPa was applied. After the dwell time, the axial pressure was released and the samples were cooled down with 100 K min<sup>-1</sup>, schematically shown in **Figure 1**.

## 2.3. Microstructural Analysis

Microstructural analysis was performed using a digital microscope VHX-6000, a laser scanning microscope from Keyence type VK-X200 series, and a scanning electron microscope Nova NanoSEM 450 from FEI. Therefore, representative cross sections of the sintered samples were embedded, ground, and polished using diamond suspensions up to a final polishing step with a particle diameter of 0.25 μm. The microstructural features were then investigated to link the macroscopic properties to the microscopic scale.

## 2.4. Electrical Conductivity

The produced materials were investigated regarding the densification and the electrical conductivity depending on the refractory metal content as well as the used starting powders. Density measurements were performed according to the Archimedes principle. The sample mass in a dry state, the apparent mass of the immersed sample, and the mass of the soaked sample were measured.

For the electrical conductivity measurement, the sample surfaces were prepared as follows: first, the sample surface was ground with SiC papers up to a grit size of P600 to produce a clean and plane surface for the deposition of an electrode. After grinding, the sample surface was sputter coated with gold, using a Quorum Q150T ES. To ensure a continuous electrode covering the whole sample surface, also in case of a certain amount of porosity, an additional layer of Pelco Colloidal Silver (Plano GmbH, Wetzlar, Germany) was added. The investigations were performed using a four-point measurement setup, also used in the study by Zienert et al.<sup>[11]</sup> During the tests, currents of 1, 10, and 100 mA were applied to the specimens using a Keithley 220 Programmable Current Source and the resulting voltages were measured with a Keithley 2000 Multimeter.<sup>[11]</sup> According to Equation (1)

$$R = \frac{U}{I} \quad (1)$$

the resistance  $R$  of the samples was calculated, where  $I$  is the applied current and  $U$  is the resulting voltage.<sup>[14]</sup> The specific resistance  $\rho$  is calculated according to Equation (2).<sup>[14]</sup>

$$\rho = \frac{R \cdot A}{l} \quad (2)$$

Here,  $A$  is the surface area of the prepared electrode and  $l$  the distance between the prepared electrodes on the sample surfaces.

## 3. Results and Discussion

### 3.1. Starting Materials

Laser scanning microscope and SEM images of the starting powders used in these studies are shown in **Figure 2**.

Figure 2 shows representative images of the differences between the particle sizes of the starting powders. From particle size distributions measured using laser diffraction and dynamic image analysis, the characteristic values  $d_{10}$ ,  $d_{50}$ , and  $d_{90}$  are extracted and listed in **Table 1**. The Nb powder shows coarse particles with a  $d_{50}$  of 37.57 μm and edges that seem to be plastically deformed. In comparison, the coarse-grained alumina Alodur with a  $d_{50}$  of 95.78 μm shows particles with sharp edges. The fine-grained alumina powder CT9FG shows way smaller particles compared with the other starting powders with a  $d_{50}$  of 4.35 μm, but it also contains agglomerates and aggregates with

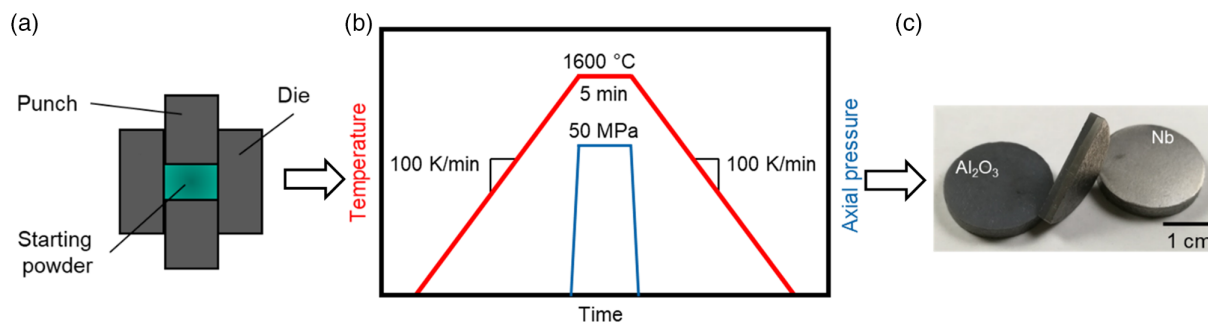


**Figure 1.** Sample preparation using FAST: a) Powder filling into punch-die setup of FAST system; b) sintering parameters; c) samples after FAST.

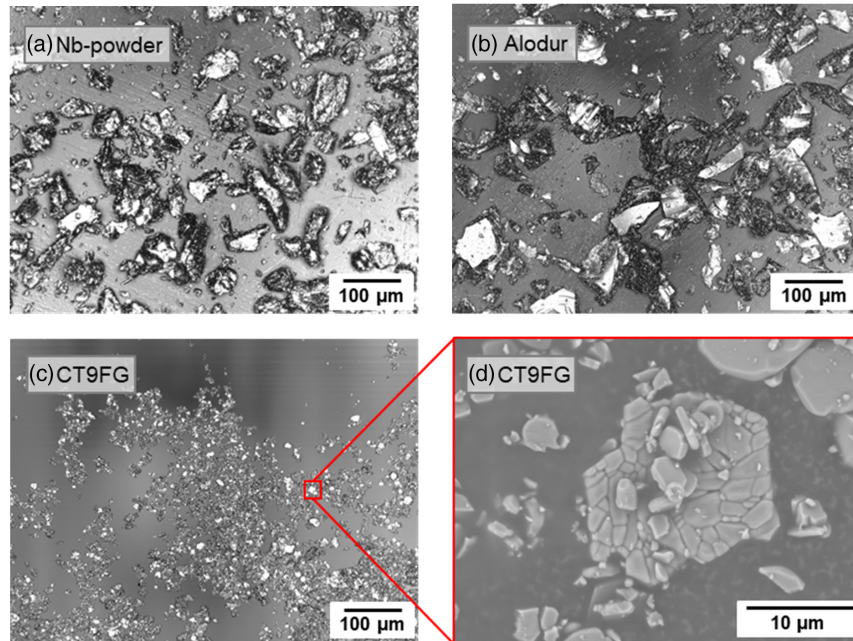


**Figure 2.** Laser scanning microscopy images of a) Nb powder (20×), b) coarse-grained alumina Alodur (20×), c) fine-grained alumina CT9FG (20×), and SEM image of d) CT9FG agglomerate (5000×).

**Table 1.** Characteristic values of particle size distribution of the used niobium and alumina (CT9FG, Alodur) starting powders.

Starting powder	$d_{10}$ [μm]	$d_{50}$ [μm]	$d_{90}$ [μm]
Nb	10.79	37.57	78.55
Alodur	44.83	95.78	162.35
CT9FG	0.76	4.35	11.93

a diameter in the range of 8–24 μm, visible in the representative SEM image shown in Figure 2.

### 3.2. Microstructural Analysis

Figure 3 shows the microstructures of Nb-CT9FG and Nb-Alodur composites with a niobium content of 20 vol%. In the laser scanning microscope images, the differences in niobium particle shape and alumina grain size can be seen.

For the composite Nb-CT9FG with the fine-grained alumina, the niobium particles (bright areas) are surrounded by sintered alumina (gray areas) particles, have an elliptical shape, and seem to be isolated from each other. In addition to the two phases niobium and alumina, a certain amount of porosity (dark areas) is visible.

Compared with the Nb-CT9FG composite, the microstructure of Nb-Alodur differs a lot. The materials' porosity strongly increases for the use of the coarse-grained alumina Alodur, compared with the fine-grained alumina CT9FG. No significant change in size and shape of the coarse alumina particles is observed during sintering of the composite. What can also be seen is that the niobium particles are plastically deformed during FAST. Niobium seems to be squeezed into the pores between the alumina particles, forming thin pathways through these pores

and possibly increasing the probability of the formation of a continuous metal network. This is also indicated in Figure 4, with a dotted red line for a composite with a very low Nb content of 10 vol% for Nb-Alodur. Further investigations are planned to clarify this phenomenon in more detail.

The formation of a continuous network would directly influence the electrical properties, namely, the percolation threshold, of the composite material. The strong dependence of percolation threshold on particle size and especially particle shape is also stated in other publications.<sup>[15–19]</sup>

The results in Figure 5 show that for the powder mixtures Nb-CT9FG, all the samples reach a high densification between 98 and 100% relative density. For the sample Nb-Alodur, the sample with Nb content of 7.5 vol% shows a relative density of 84.1%, increasing with an increase in refractory metal content up to a value of 98.5% relative density for the sample with 80 vol% niobium.

The cross section of the Nb-CT9FG composite with a composition of 20 vol% niobium and 80 vol% alumina is shown in Figure 6. On the left side, the orientation of the cross section relative to the pressure direction during FAST process is illustrated and is also indicated by the letters “L” and “R”. What can be clearly seen is that as a result of applying a pressure on the powder filling during FAST an anisotropy of the components is caused. The visible grains are elongated perpendicular to the pressure direction.<sup>[2]</sup> This anisotropy can be seen for all material compositions independent of the alumina particle size or amount of porosity.

### 3.3. Electrical Conductivity Measurement

In Figure 7, the results of the electrical conductivity measurements are shown. As the porosity influences the electrical

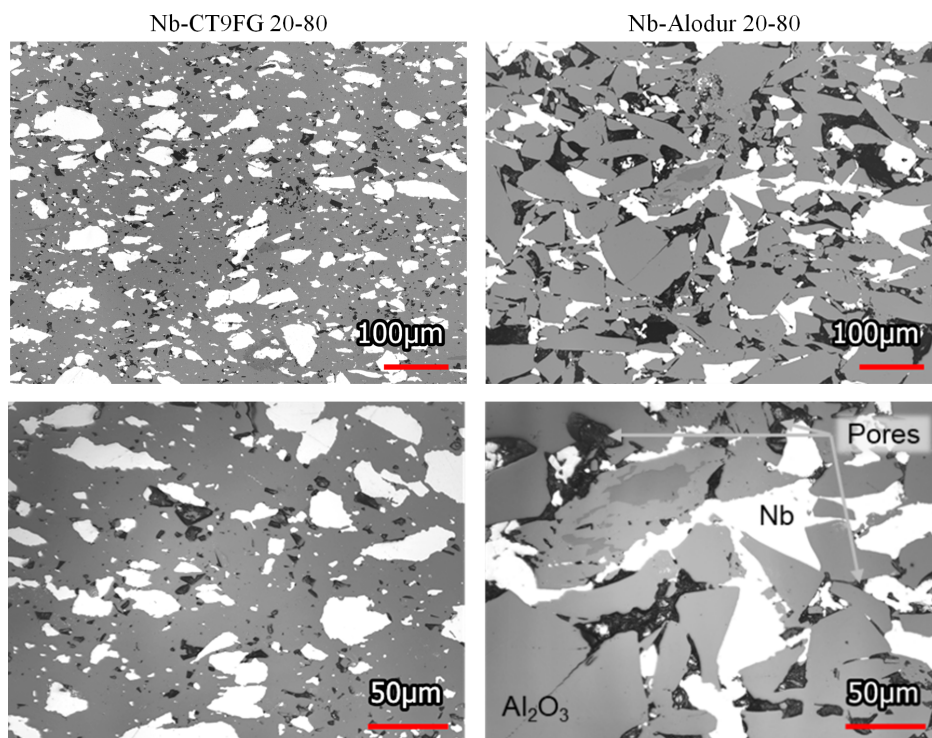


**Figure 3.** Laser scanning microscope images of Nb-CT9FG (left) and Nb-Alodur (right) composite material with 20 vol% niobium content after sintering with magnification of 20× (upper images) and 50× (lower images).

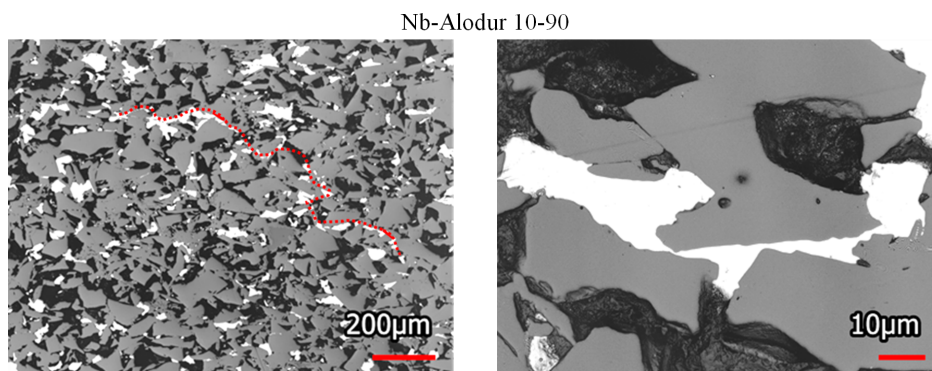


**Figure 4.** Laser scanning microscope images of Nb-Alodur indicating the possible formation of an electrically conductive network by plastic deformation of niobium particles during FAST, at magnifications of 10× (left) and 150× (right).

conductivity, the densities were also plotted for all measured samples.

For both composite materials, the electrical conductivity increases with increasing Nb content. Up to a volume fraction of 40%, the electrical conductivity of the material system with the coarse-grained alumina Nb-Alodur increases faster compared with the material system with the fine-grained alumina Nb-CT9FG. For the compositions with  $\geq 60$  vol% niobium, the electrical conductivity of the composite materials is similar. The percolation threshold for Nb-CT9FG composites can be found at 17.5 vol% niobium, which is in good agreement with percolation theory of particle composites.<sup>[15–17]</sup> The percolation

threshold of niobium in combination with the coarse-grained alumina Alodur is found to be at 10 vol% niobium.

According to literature, the electrical conductivity of a material decreases with increasing porosity, which is in contrast to the results found in this study.<sup>[20–22]</sup> Here the influences of relative particle size and particle shape seem to be the predominant factors when it comes to the formation of a conducting network in the composite material. Especially the particle aspect ratio is reported to influence the percolation threshold, making it possible to reduce the amount of conducting phase used.<sup>[5,15,16,23,24]</sup>

For pure Nb, an electrical conductivity of  $1.78 \times 10^4 \text{ S cm}^{-1}$  is measured. This result is slightly smaller than the values of

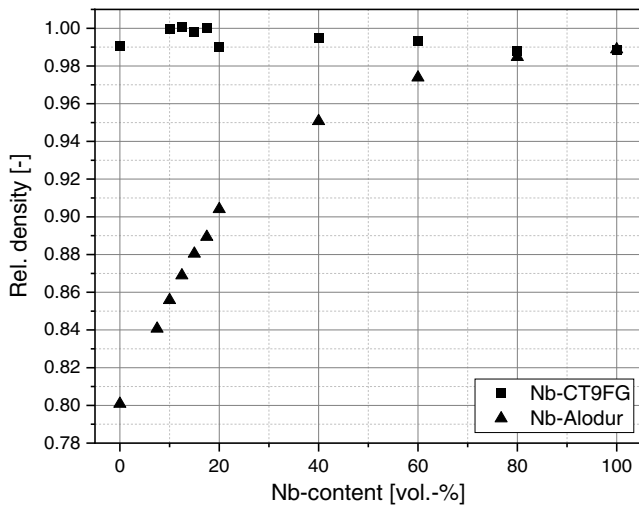


**Figure 5.** Relative density of Nb-CT9FG and Nb-Alodur composite materials with different volume contents of Nb.

$5.9\text{--}6.8 \times 10^4 \text{ S cm}^{-1}$ , reported in the study by Shabalin et al.<sup>[25]</sup>. A reason for these results may be secondary phases, like

niobium oxides, detectable within the microstructure of the niobium and the X-ray diffraction (XRD) pattern of the starting powder, shown in **Figure 8**.

The aforementioned influence of the anisotropy effect on material properties is shown in **Figure 9**. The electrical conductivity along the *a*-axis is slightly smaller compared with the electrical conductivity along the *b*- and *c*-axis. (The value measured along the *c*-axis for the sample with 40 vol% Nb is considered a measurement error.) This effect of anisotropy is caused by the elongation of the particles perpendicular to the pressure direction. This difference in the aspect ratio leads to an increasing probability of formation of conducting pathways and therefore a higher conductivity of the material in these directions.

This effect caused by the processing route, in this case FAST, has to be taken into account when investigating electrical or mechanical material properties.

#### 4. Conclusion

This study is part of the interdisciplinary Research Group FOR 3010 dealing with the investigation of coarse-grained refractory composite materials. The main goal is the production of materials by a newly developed two-step process. First the starting

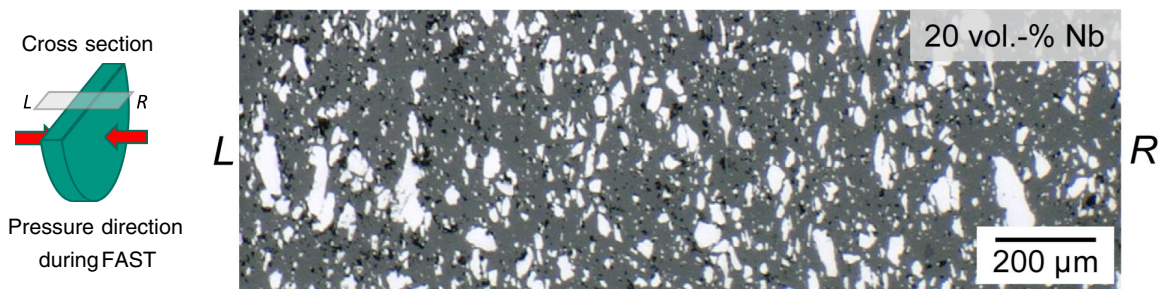


**Figure 6.** Digital microscopy images of cross sections of Nb-CT9FG 20–80 composite with orientation relative to pressure direction during FAST, magnification of 100 $\times$ .

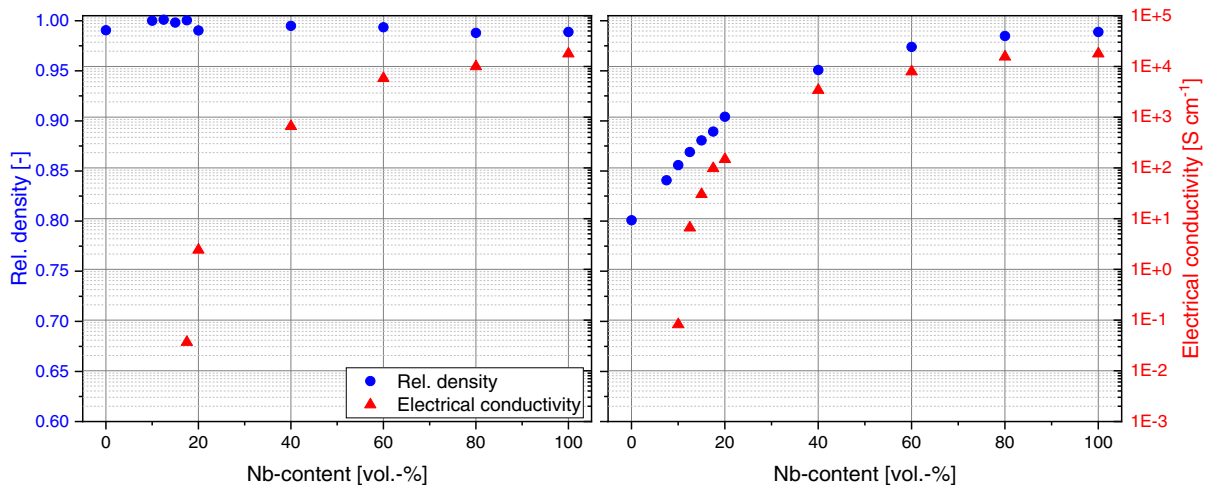


**Figure 7.** Rel. density and electrical conductivity of niobium in combination with the fine-grained alumina Nb-CT9FG (left) and in combination with the coarse-grained alumina Nb-Alodur (right) composites depending on Nb content.

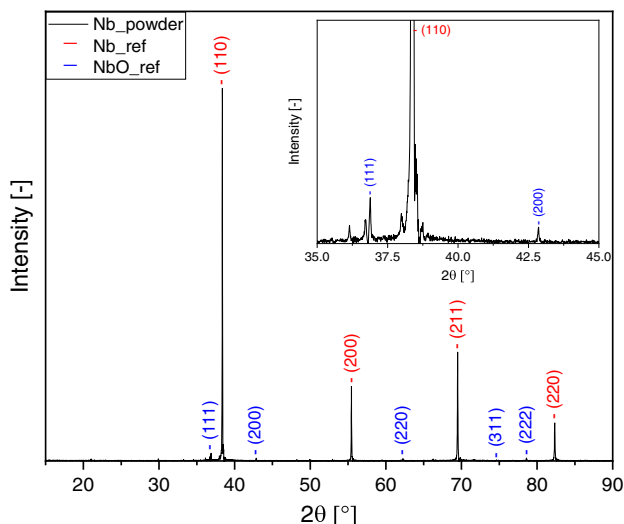
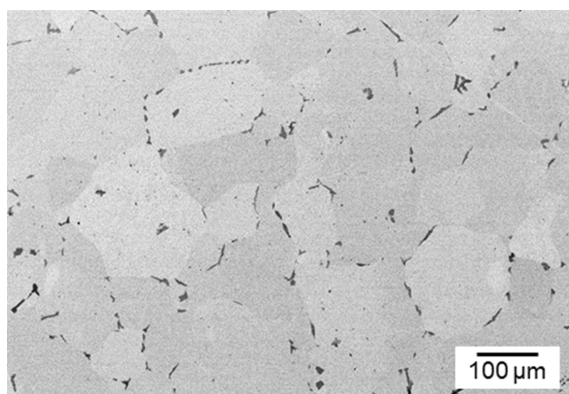


**Figure 8.** SEM image of niobium sample (magnification 500×) with secondary phases (darker areas) detectable at Nb grain boundaries (top) and XRD pattern of Nb starting powder including Nb and NbO reference (below).<sup>[26,27]</sup> For better visibility of NbO, an enlarged graph is displayed for the  $2\theta$  section between 35° and 45°.

materials are needed for the production of coarse-grained granules, which are then used for production of coarse-grained composite materials specifically designed for different high-temperature applications. For use at high-temperature coarse grains, a certain amount of porosity and specific electrical conductivity result in low shrinkage during sintering, good creep and thermal shock resistance, and adjustable electrical properties depending on the material composition.<sup>[10–13]</sup> Here, a first study was executed to find out about the densification behavior during processing as well as the influence of the parameter “alumina particle size” on percolation threshold and microstructural features.

Important findings of the study are the processing of the fine-grained starting powders for production of dense composites, which in further progress can be used as dense granules for the second step of the processing route. We could show that the coarse-grained alumina already leads to a certain amount of porosity, which might be favorable for thermal shock behavior and at the same time decrease the percolation threshold to smaller amounts of niobium, resulting in lower costs if the electrical conductivity is of major importance compared with density.

## 5. Summary

In this study, Nb–Al<sub>2</sub>O<sub>3</sub> composite materials were successfully prepared using FAST. Two alumina powders with different particle sizes were used and the influence on the microstructure and electrical conductivity was investigated. The fine-grained alumina samples have a relative density >98% for all compositions, while for the coarse-grained alumina the density increases from 84.1% relative density for the sample with 7.5 vol% Nb to 98.5% relative density of the sample with 80 vol% Nb.

It was also found that for the fine-grained alumina the percolation threshold is at 17.5 vol% niobium and for the coarse-grained alumina at 10 vol% niobium. The difference

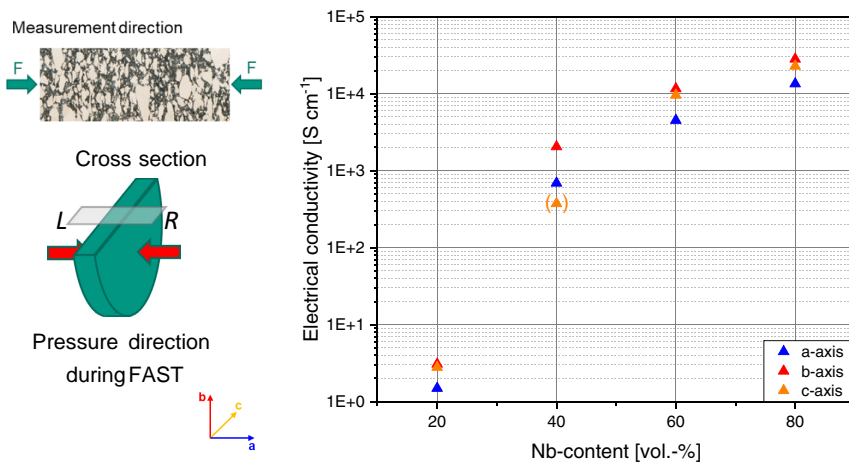


**Figure 9.** Electrical conductivity of Nb-CT9FG in different directions relative to pressure direction during FAST. a) Axis parallel to pressure direction. b, c) Axis perpendicular to pressure direction.

in percolation threshold can be explained by the microstructure of the investigated materials. For the coarse-grained alumina, the electrically conductive niobium grains deform plastically during FAST process and therefore the aspect ratio of the shape increases. This increase in aspect ratio leads to a higher probability of formation of a conducting network through the composite material. With increasing refractory metal content, the electrical conductivity increases for both material systems. It was also found that the FAST process results in anisotropy, with particles elongated perpendicular to the pressure direction during sintering. This leads to anisotropic electrical properties of the composite materials, with slightly increased electrical conductivity in the direction perpendicular to the pressure direction during the FAST process.

This study was carried out to get a basic understanding of the investigated materials. The most promising materials will be used for the fabrication of granules for the preparation of coarse-grained refractory composites. Based on the results found here, the material compositions with high densification in combination with a low Nb content are of great interest. Also, the composites with the lowest possible niobium content while still achieving electrical conductivity are promising materials for further investigations of the Research Unit FOR 3010.

## Acknowledgements

This research was funded by the German Research Foundation (DFG) within the Research Unit FOR 3010 (project number: 416817512). Thanks to Madlen Müller from TU Bergakademie Freiberg for technical support.

Open Access funding enabled and organized by Projekt DEAL.

## Conflict of Interest

The authors declare no conflict of interest.

## Data Availability Statement

The data that support the findings of this study are available from the corresponding author upon reasonable request.

## Keywords

alumina, electrical conductivity, field-assisted sintering, niobium, refractory composites

Received: January 13, 2022  
Revised: May 11, 2022  
Published online: May 31, 2022

- [1] M. K. L. Feuchter, *Investigations on Joule heating applications by multi-physical continuum simulations in nanoscale systems*, KIT Scientific Publishing, Schriftenreihe des IAM, Band 43, Karlsruhe **2014**.
- [2] O. Guillon, J. Gonzalez-Julian, B. Dargatz, T. Kessel, G. Schierning, J. Räthel, M. Herrmann, *Adv. Eng. Mater.* **2014**, *16*, 830.
- [3] J. Räthel, M. Herrmann, W. Beckert, *J. Eur. Ceram. Soc.* **2009**, *29*, 1419.
- [4] K. Vanmeensel, A. Laptev, J. Hennicke, J. Vleugels, O. Van Der Biest, *Acta Mater.* **2005**, *53*, 4379.
- [5] M. Sahimi, A. G. Hunt, *Complex Media and Percolation Theory*, 1st ed., Springer Science+Business Media New York, New York, **2021**.
- [6] D. Aronov, M. Molotskii, G. Rosenman, *Appl. Phys. Lett.* **2007**, *90*, 104104.
- [7] R. Shamaï, D. Andelman, B. Berge, R. Hayes, *Soft Matter* **2007**, *4*, 38.
- [8] G. Lippmann, *Relations entre les phénomènes électriques et capillaires*, Academic Thesis, France, Université, Paris, **1875**.
- [9] A. Froumkine, *Actual. Sci. Ind.* **1936**, *373*, 5.
- [10] C. G. Aneziris, M. Hampel, *Int. J. Appl. Ceram. Technol.* **2008**, *5*, 469.
- [11] T. Zienert, D. Ender, J. Hubáľková, *Materials* **2021**, *14*, 6453.
- [12] T. Zienert, M. Farhani, S. Dudczig, C. G. Aneziris, *Ceram. Int.* **2018**, *44*, 16809.
- [13] A. Weidner, Y. Ranglack-Klemm, T. Zienert, C. G. Aneziris, H. Biermann, *Materials* **2019**, *12*, 3927.
- [14] M. E. Orazem, B. Tribollet, *Electrochemical Impedance Spectroscopy*, 2nd ed., John Wiley and Sons, Hoboken, NJ **2017**.
- [15] Q. Xue, *Eur. Polym. J.* **2004**, *40*, 323–327.
- [16] X. Jing, W. Zhao, L. Lan, *J. Mater. Sci. Lett.* **2000**, *19*, 377.
- [17] S. H. Yao, Z. M. Dang, M. J. Jiang, H. P. Xu, L. Lan, *Appl. Phys. Lett.* **2007**, *91*, 212901.
- [18] Z. M. Dang, J. P. Wu, H. P. Xu, S. H. Yao, M. J. Jiang, J. Bai, *Appl. Phys. Lett.* **2007**, *91*, 2005.
- [19] R. H. Schmidt, I. A. Kinloch, A. N. Burgess, A. H. Windle, *Langmuir* **2007**, *23*, 5707.
- [20] N. Probst, E. Grivei, *Carbon* **2002**, *40*, 201.
- [21] L. J. Kennedy, J. J. Vijaya, G. Sekaran, *Mater. Chem. Phys.* **2005**, *91*, 471.
- [22] H. El Khal, A. Cordier, N. Batis, E. Siebert, S. Georges, M. C. Steil, *Solid State Ionics* **2017**, *304*, 75.
- [23] A. K. Sircar, T. G. Lamond, *Rubber Chem. Technol.* **1978**, *51*, 126.
- [24] R. G. Arenhart, G. M. O. Barra, C. P. Fernandes, *Polym. Compos.* **2016**, *37*, 61.
- [25] I. L. Shabalín, *Ultra-High Temperature Materials I*, 1st ed., Springer Netherlands, Dordrecht, **2014**.
- [26] R. Roberge, *J. Less-Common Met.* **1975**, *40*, 161.
- [27] O. Kubaschewski, *J. Less-Common Met.* **1960**, *2*, 172.